Understanding Temperature Dependency of Hydrogen Solubility in Ionic Liquids, Including Experimental Data in [bmim][Tf_2N]

Sona Raeissi
School of Chemical and Petroleum Engineering, Shiraz University, Shiraz 71345, Iran

Cor J. Peters
Dept. of Process and Energy, Faculty of Mechanical, Maritime and Materials Engineering, Laboratory of Process Equipment, Delft University of Technology, Leeghwaterstraat 44, 2628 CA Delft, The Netherlands; The Petroleum Institute, Chemical Engineering Dept., Abu Dhabi, United Arab Emirates, and Dept. of Chemical Engineering and Chemistry, Separation Technology Group, Eindhoven University of Technology, Eindhoven, The Netherlands

DOI 10.1002/aic.13742
Published online February 21, 2012 in Wiley Online Library (wileyonlinelibrary.com).

Previously unavailable high-pressure solubility data of hydrogen in 1-butyl-3-methylimidazolium bis(trifluoromethylsulfonyl)amide has been measured experimentally up to temperatures and pressures of 450 K and 15 MPa, respectively. In contrast to CO_2 solubility, H_2 tends to dissolve better in the ionic liquid at higher temperatures. This ''inverse'' temperature effect has been studied from a thermodynamic perspective and the underlying reason for this effect is explained. It is shown that the negative P-T *slope is not limited to this particular binary mixture, but is the typical behavior in most, if not all, H_2 + ionic liquid systems. However, there is a certain range of temperatures, pressures, and concentrations in which this phenomenon occurs. By predicting the Scott-van Konynenburg phase diagram for systems of H_2 + ionic liquids to be of type III, it is shown how and why the solubility increases with temperature in some regions, but decreases in others.* © 2012 American Institute of Chemical Engineers *AIChE J,* 58: 3553–3559, 2012
Keywords: 1-butyl-3-methylimidazolium bis(trifluoromethylsulfonyl)imide, 1-butyl-3-methylimidazolium bis(trifluoromethyl sullfonyl)amide, H_2, phase equilibria, vapor-liquid equilibria

Introduction

One of the grand challenges of this century is to supply energy to meet the changing needs of a growing population in a way that protects the environment. The use of hydrogen as fuel is among the strategies being investigated. This study is part of the general research scheme[1] of hydrogen production using separation-enhanced reactors in which the carbon dioxide byproduct in hydrogen formation is separated through a supported ionic liquid membrane. However, the interest in hydrogen solubility in an ionic liquid (IL) is by no means limited to the aforementioned application. Applications of ionic liquids in hydrogenation and hydroformylation, and also in fuel cell and electrochemical technology are some of the current research topics which also require accurate knowledge of H_2 + IL phase behavior.[2]

This study uses an experimental approach to obtain the solubility of H_2 in 1-butyl-3-methylimidazolium bis(trifluoromethylsullfonyl)amide, usually abbreviated to [bmim][Tf_2N]. Jacquemin et al.[3] measured the phase behavior of this system close to atmospheric pressures. However, to the best of our knowledge, no experimental data is available in open literature on the high-pressure phase behavior of this particular binary system. In addition, due to the necessity to have a thorough understanding of the solubility of hydrogen in ILs, especially since such systems have a temperature dependency which is the opposite of commonly studied gases such as CO_2, we have tried to explain the thermodynamic basis for this behavior and to present the global phase diagram of H_2+ IL. The identification of the type of Scott-van Konynenburg phase diagram[4] is of great importance as it can help us to predict, qualitatively, the number of phases, the types of phases and the critical phenomena that may be expected of such systems outside of the regions investigated so far by experimentalists. In addition, such knowledge can also assist laboratories in selecting the temperature and pressure ranges of interest to them for further experimentation, and to prevent misinterpretations of their measured data.

Experimental

A synthetic method of phase equilibria measurement was employed. A mixture having a constant overall composition of hydrogen and [bmim][Tf_2N] is injected into an equilibrium cell using an equipment called a ''gas rack''[5] At any desired temperature (up to 450 K), the pressure is increased (up to 15 MPa), while stirring the sample, until the dissolution of the last bubble of gas in the ionic liquid is observed

Correspondence concerning this article should be addressed to S. Raeissi at raeissi@shirazu.ac.ir.

Table 1. Experimentally Measured Solubility Data (bubble-point curves) for Hydrogen in [bmim][Tf_2N]

Mole % CH_4	T, K	P, MPa	T, K	P, MPa	T, K	P, MPa
2.12	313.48	4.538	332.68	4.213	352.11	3.813
	371.44	3.540	390.83	3.215	410.29	3.075
	429.78	2.865	449.30	2.690		
2.83	323.11	5.292	332.71	5.057	342.41	4.843
	352.14	4.632	371.49	4.258	390.90	3.983
	410.49	3.709	429.85	3.459	449.40	3.260
3.50	313.56	7.504	323.05	7.153	342.41	6.529
	361.84	6.053	381.24	5.604	400.74	5.204
	420.17	4.879	439.71	4.579	449.42	4.454
5.16	313.59	11.253	323.05	10.653	342.40	9.753
	361.83	8.953	381.21	8.278	400.79	7.728
	420.20	7.253	439.73	6.778	449.46	6.554
7.35	352.18	13.505	371.56	12.505	390.96	11.580
	410.44	10.856	429.94	10.156	449.42	9.531
8.52	380.73	14.154	390.45	13.628	400.30	13.103
	410.11	12.553	424.79	11.903	436.89	11.379
	449.42	10.929				
9.37	420.14	14.105	429.83	13.606	439.52	13.206
	449.25	12.706				
10.81	440.59	15.434	442.82	15.327	444.52	15.302
	447.94	15.227	449.40	15.202		

visually. The equilibrium cell is called the Cailletet tube which is essentially a thick-walled Pyrex glass tube with one open end. A sample of a fixed known composition is confined over mercury in the sealed end this tube. The open end is immersed in mercury within an autoclave. In this manner, mercury serves as both sealing the sample in the equilibrium cell and transmitting pressure to the sample. The autoclave is connected to a hydraulic oil system which generates the desired pressure by means of a screw-type hand pump. This pressure is measured with the aid of a dead-weight pressure gauge. The Cailletet tube is inserted within a glass thermostat jacket. Thermostat liquid, whose temperature is controlled by a thermostat bath with a constancy better than ± 0.01 K, is circulated within this jacket to establish the desired temperature in the sample. This temperature is measured with the aid of a platinum resistance thermometer, located close to the sample-containing part of the Cailletet tube. To ensure adequate mixing of the sample to reach equilibrium, a stainless steel ball is initially placed inside the fluid sample, which is activated by reciprocating magnets when stirring of phases is required. The schematic diagram of the apparatus and further details of the experimental procedure are given elsewhere.[5–7] The uncertainties of measurement were within 0.03% of the reading for pressure, 0.02 K for temperature, and 0.001 for mole fraction. Hydrogen and [bmim][Tf_2N] were purchased from Hoek Loos and Fluka

Table 2. Interpolated Isothermal Solubility Curves for Hydrogen in [bmim][Tf_2N]

H_2 Mole% T, K	2.12 P, MPa	2.83 P, MPa	3.5 P, MPa	5.16 P, MPa	7.35 P, MPa	8.52 P, MPa	9.37 P, MPa	10.81 P, MPa
333.15	4.165	5.046	6.830	10.168				
353.15	3.813	4.612	6.255	9.278	13.455			
373.15	3.504	4.247	5.768	8.548	12.409			
393.15	3.237	3.937	5.354	7.940	11.516	13.472		
413.15	3.011	3.670	4.997	7.417	10.741	12.434		
433.15	2.824	3.434	4.682	6.937	10.053	11.529	13.478	
453.15	2.676	3.216	4.394	6.464	9.415	10.814	12.531	15.202

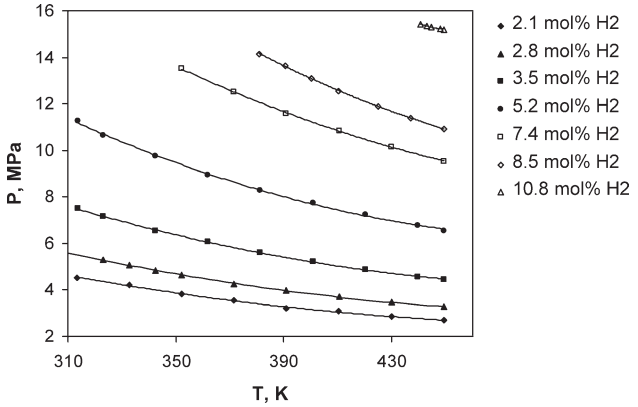

Figure 1. Experiemntal pressure-temperature results for binary mixtures of H_2 + [bmim][Tf_2N] with varying concentrations.

and had purities of 99.9990% and $\geq$98%, respectively. The ionic liquid was dried with molecular sieves *in vacuo* for several days prior to use.

Results

Table 1 presents the experimentally measured solubility limits of H_2 in [bmim][Tf_2N] at various temperatures and pressures, but constant compositions, while Table 2 gives a more useful form of the data as isotherms, interpolated from the data of Table 1. Figures 1 and 2 graphically show the directly measured *P-T* and interpolated *P-x* solubility curves, respectively. Solubility results confirmed our expectation of low-hydrogen solubility in [bmim][Tf_2N], even at high pressures. The maximum amount of hydrogen that could be dissolved in the ionic liquid within the temperature and pressure limits of our experimental apparatus was about 10 mole percent (at a pressure of about 15 MPa and 453 K). The solubility increased with increasing pressure and the variation was rather linear. However, whereas most systems show a decrease in gas solubility upon temperature increase, hydrogen exhibits the opposite trend in [bmim][Tf_2N], as witnesses by the downward slope of the isopleths in Figure 1.

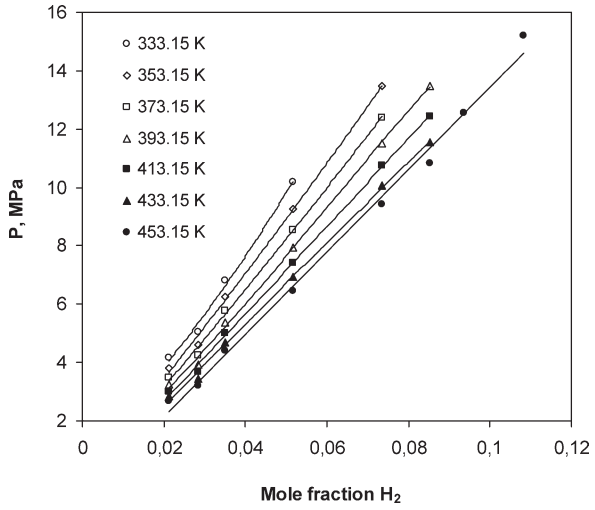

Figure 2. Interpolated pressure-composition isotherms for the system of H_2 + [bmim][Tf_2N] with varying concentrations.

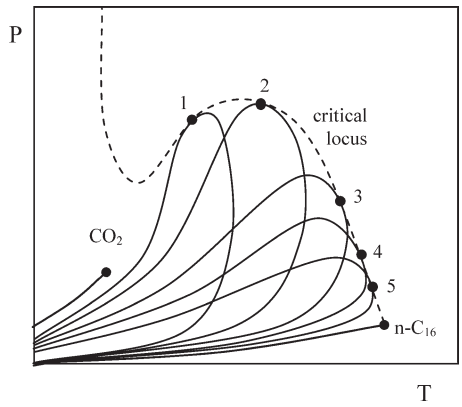

Figure 3. Schematic presentation of *P-T* phase envelopes and critical locus for the binary mixture CO_2 + n-C_{16}.

The same trend has been observed for the solution of hydrogen in other members of this homologous family[1,8] (1-ethyl-3-methylimidazolium bis(trifluoromethylsulfonyl)amide and 1-hexyl-3-methylimidazolium bis(trifluoromethylsulfonyl)amide), as well as in ionic liquids with differing anions such as, for example, 1-butyl-3-methylimidazolium hexafluorophosphate, 1-butyl-3-methylimidazolium tetrafluoroborate and 1-butyl-3-methylimidazolium methyl sulfate.[9,10,11] In the next section, the thermodynamic reasoning for this seemingly general behavior in ionic liquids will be explained.

The collective results of the experimental work done in our laboratory[1,7,8,12] have confirmed the high solubilities of CO_2, and low solubilities of H_2 in the 1-alkyl-3-methylimidazolium bis(trifluoromethylsulfonyl)amide family of ionic liquids. It is shown that the solubility of hydrogen is one order of magnitude lower than the corresponding solubility of CO_2 in [bmim][Tf_2N]. A ratio of CO_2/H_2 up to 15 has been observed within the operating limits of the experimental apparatus,[1] opening up the doors for further investigation on the hypothesis of using ILs as potential gas separation media, at least from the point of view of solubility differences.

Thermodynamic explanation of temperature dependency

A schematic presentation of the phase behavior of a binary system differing greatly in molecular size and/or structure and/or chemical nature, namely CO_2 + n-C_{16}, is presented in Figure 3.[13,14] Several typical phase envelopes are shown in this figure, with the bubble-point curve and the dew-point curve coming together at the critical point, shown by the filled circle. The critical points of these mixtures are connected together to make the dashed critical locus curve. Thermodynamics dictates that the critical locus is tangent to the *P-T* diagrams at the critical point of each mixture, since it defines the upper limit of the liquid-vapor region. Because of this, and due to the fact that the critical locus curve approaches its end at the pure heavy component critical point with a rather large negative slope for this binary system, as the concentration of the heavy component increases in the mixtures, the critical point moves more and more to the right on the phase envelope, passes the "nose" (as shown by curve 2 in Figure 3), and ultimately moves toward the lower branch of the phase envelope as shown for envelopes 3, 4, and 5 on Figure 3. While the more volatile mixtures such as that shown by curve 1, have positive-sloped bubble-point curves all throughout up to the critical point on the *P-T* diagram, the less-volatile mixtures such as those shown by curves 3, 4, and 5, have a region approaching the critical point, in which the bubble-point curve has a negative slope. If the critical temperatures of the two pure components making up the mixture are further and further removed from one-another, it is expected that the negative-sloped part of the bubble-point curve increases its span.

Although not the same type of phase behavior, for the sake of easier understanding, the phase behavior of hydrogen + ionic liquids can, in a way, be explained using that of CO_2 + n-C_{16}. The extremely small and light hydrogen molecules are highly different from heavy ionic liquid ion pairs. Hydrogen has a critical temperature of 33.2 K. This is in high contrast to ionic liquids which have predicted critical temperatures[15] in the range of 500–1,500 K. This large difference in critical points would, in analogy to what is mentioned previously, result in a very large temperature range in which the bubble-point curve has a negative slope within the low concentrations that hydrogen dissolves in ionic liquids. The temperature range with negative-sloped bubble-point curves is, in fact, so large that it easily covers and goes beyond the span of experimental data usually measured for hydrogen solubilities in different *PVT* laboratories, i.e., from ambient temperatures up to several hundred Kelvins. Körösy[16] has suggested that the temperature coefficient of solubility at constant pressure is positive for gases with critical temperatures below 180 K, and negative for those with T_C above 180 K. Although this is an over-generalized statement since it does not take into account the nature of the solvent, it does in a way confirm our idea based on widely differing critical temperatures.

Carbon dioxide, on the other hand, has a critical temperature of 304.4 K. If the gases H_2 and CO_2 are compared in binary mixtures with ionic liquids, it is immediately evident that the temperature span on the Scott-van Konynenburg diagrams[4] between the gas vapor pressure curve and the ionic liquid vapor pressure curve is about 270 K larger for H_2 than that of CO_2. So, while H_2 mixtures easily fall in the very large negatively-sloped *P-T* region at laboratory conditions, CO_2 mixture data usually do not fall in the much smaller (if any at all) negative-sloped region, and, therefore, show the more conventional positive slope.

It is obvious that the aforementioned discussion would be easier understood if we could experimentally determine the Scott-van Konynenburg diagram for hydrogen + IL systems. Unfortunately up to date, this is not possible since no data is available for such binary mixtures close to critical points of neither hydrogen nor the IL. The former requires cryogenic temperatures and the latter is basically impossible to reach, not only because the critical temperatures of many ionic liquids are in the range of a thousand Kelvins, but because most ILs thermally degrade before reaching their critical temperatures. So there is little hope that laboratories will be able to provide us with the information necessary to plot the critical loci projections over the whole range between the two pure component critical points. However, a speculation of the type of phase behavior is possible. We expect H_2+ IL systems to have type III phase behavior according to the classification of Scott-van Konynenburg,[4] as shown in Figure 4 with two critical loci (dotted lines), instead of one uninterrupted critical curve running from the critical point of hydrogen to the IL.

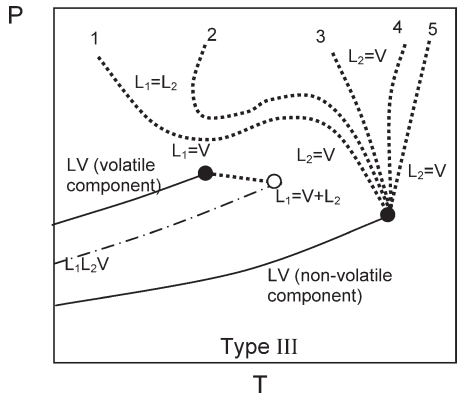

Figure 4. Schematic diagram for Type III phase behavior showing the different shapes and trends that the projected mixture critical loci can have.

Type III phase behavior can have various shapes for the critical locus[17] starting at the IL critical point, as shown in Figure 4 by branches 1 through 5. The exact shape will depend on the specific ionic liquid involved, but we expect that it may behave similar to branches 3 or 4 with the critical locus running to infinitely high pressures, but more probably somewhere in the middle with a near-vertical slope. Experimental evidence of binary systems of hydrogen with normal alkanes[18–20] and with methanol[21] has branch 3-type behavior as shown in Figure 5. This figure is plotted as reduced temperature and pressure so that the different solvents with differing critical properties can be easily compared at one point representing all their critical points. The molecular/structural differences between H_2, and these solvents is less than between H_2 and ILs. It is known that as molecular differences increase, the critical branches tend to shift even further to the right, so it is possible that H_2 + IL critical loci fall in the shaded region of Figure 5.

From the aforementioned explanations, it is evident that the increase of solubility with temperature is limited to certain spaces on the *P-T-x-y* diagram. In fact, Jacquemin

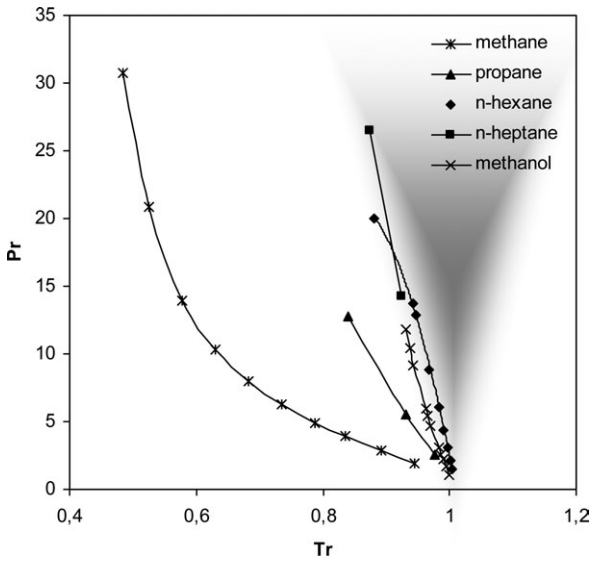

Figure 5. Experimentally determined critical loci of binary mixtures of hydrogen + solvent.

Data are taken from Refs. 18–21.

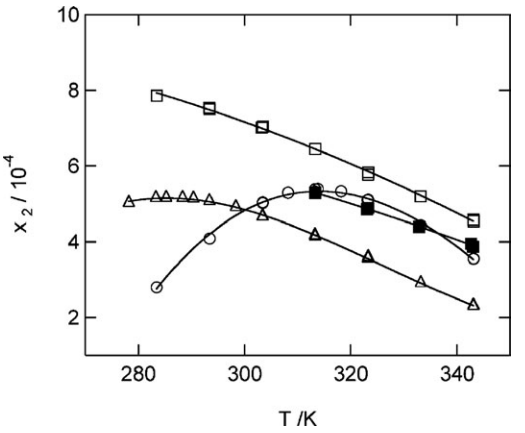

Figure 6. Change of temperature-dependency of hydrogen solubility in some ionic liquids: □, [bmim][Tf_2N]; ■,[bmim][C_8SO_4]; ○[bmim][PF_6], Δ, [bmim][BF_4].

Reproduced by permission of The Royal Society of Chemistry.[22]

et al.[10,22,23] have presented experimental evidence where the solubility of hydrogen at nearly atmospheric pressure has a decreasing trend with temperature in the ionic liquids [bmim][C_8SO_4] or [bmim][Tf_2N], but an increasing-then-decreasing trend in [bmim][PF_6], in [bmim][BF_4] and in [emim][C_2SO_4]. This behavior is shown in Figure 6 ([emim][C_2SO_4] not shown).

To explain the change in temperature-dependency observed for hydrogen solubility in ionic liquids, we have proposed the schematic phase behavior at constant concentrations (phase envelopes) given in Figure 7. Very low concentrations of hydrogen may have a minimum-containing bubble-point curve similar to branch 1. If one moves to higher temperatures along a constant pressure line such as at P_1, at lower temperatures the solubility increases with temperature, but after passing the minimum dip, the solubility will decrease upon further increase in temperature.

If a constant temperature path is chosen on Figure 7 such as that shown at T_1, the solubility will monotonously increase as pressure is increased. This is also confirmed by our data plotted in Figure 2.

The particular change of shape from branch 1 to 4 of Figure 7 is the consequence of the limited solubility of such a light gas in a liquid: very minor amounts of gas will dissolve in the liquid, however, to force further gas to dissolve, the

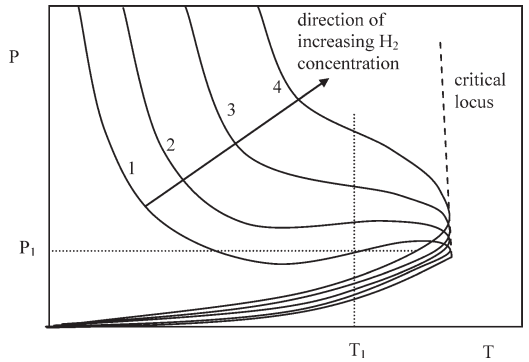

Figure 7. Proposed bubble point curves at low hydrogen concentrations in ionic liquids.

pressure must be increased excessively. However, even increasing the pressure to infinity will most likely not result in the dissolution of hydrogen to any desired proportions. We expect that H_2+IL will most probably have an immiscibility gap up to infinite pressures. Such behavior with a *P-T* minimum has been observed experimentally in other systems as well, for example, in mixtures of helium + water,[24] hydrogen + methane,[18] hydrogen + petroleum naphtha,[25] and hydrogen + ammonia.[26]

On a molecular level, a number of different mechanisms regarding molecular interactions go hand-in-hand to determine the temperature dependency of gas solubility. We speculate the observed behavior of H_2 solubility to be the result of the expansion of the ionic liquid upon heating, providing some free voids or "pockets" within the large bulky ionic liquid molecules for small hydrogen molecules to squeeze into. This effect probably dominates all other mechanisms in the case of H_2 solubility since even the slightest decrease in density resulting from a temperature increase results in very small free spaces that the extremely small hydrogen molecule can still manage to fit into, thus increasing solubility. This idea is confirmed by calculations performed by Körösy[16] from experimental data of gas solubility in organic solvents (not ionic liquids): While the temperature derivative of molar solubility at constant hydrostatic pressure $(\partial\gamma_M/\partial T)_\Pi$, where γ_M is the volume of gas dissolved in one mole solvent had positive values when dissolving hydrogen in all the organic solvents investigated, the change of hydrogen solubility at constant *volume* $(\partial\gamma/\partial T)_V$, was calculated to be negative in all the same solvents. The positive values of $(\partial\gamma_M/\partial T)_\Pi$ was the consequence of thermal expansion of the liquid, resulting in more free space available for the dissolving gas molecules with increasing temperature. However, when the volume is kept constant while temperature increases, no additional free spaces are born and the solubility derivative is negative instead.

Yet, another very simple way to understand inverse hydrogen solubility is based on Le Chatelier's principle. In an article explaining the temperature dependence of the solubility of salts, Bodner[27] also made an analogous comparison to gas solubility in a weakly interacting solvent as being equivalent to the two following steps:

$$\text{condensation}: \quad \text{gaseous solute} \xrightarrow{\Delta H_1} \text{liquid state} \tag{1}$$

$$\text{mixing}: \quad \text{liquid solute} + \text{solvent} \xrightarrow{\Delta H_2} \text{solution} \tag{2}$$

However, by reasoning that the enthalpy of mixing (ΔH_2) is negligible and the enthalpy of liquefaction of the gaseous solute is exothermic, he concluded that the enthalpy of solution of gases in weakly interacting solvents is negative, resulting in the net decrease in the solubility of most gases with increasing temperature. We can clarify this ambiguity by incorporating the concept of the Joule-Thomson effect into the reasoning. Since most gases have an inversion temperature somewhere around or above 350°C (623 K), they have a positive Joule-Thomson coefficient, μ_{JT}, at normal temperatures. This means that they will cool upon expansion, and, thus, the value of ΔH_1 is negative as Bonder[27] suggested. However, the dominating intermolecular interactions in hydrogen are repulsive rather than attractive at normal temperatures, and it is necessary to give energy to the system in order to change it into the liquid state. Therefore, above its inversion temperature of −69°C (204.15 K), the values of ΔH_1 will be positive for hydrogen. According to Le Chatelier's principle, increasing the temperature will, thus, result in the shift of the equilibrium in the direction to dissolve more and more hydrogen into the ionic liquid. It must be noted that strictly speaking, the aforementioned method of reasoning is valid for low (subcritical) pressures of hydrogen (<1.30 MPa), where pure hydrogen can actually liquefy. In a broader scope at supercritical pressures for hydrogen, one would need to look upon the first equation as the compression of supercritical fluid into a more dense state rather than actual liquefaction. In either case, as long as the temperature is higher than the inversion temperature of hydrogen, the positive values of ΔH_1 will result in negative *P-T* behavior for the binary mixture.

Starting with the equation of the equality of chemical potential of species *i* in the vapor and liquid phases at equilibrium, Wisniak et al.[28] arrived at the following equation for the variation of solubility with temperature in a binary system

$$\left(\frac{\partial x_1}{\partial T}\right)_P \approx -\frac{y_1\Delta\bar{H}_1 + y_2\Delta\bar{H}_2}{T(y_1 - x_1)}\left(\frac{\partial^2\tilde{G}^L}{\partial x_2^2}\right)^{-1}_{T,P} \tag{3}$$

where G^L is the molar Gibbs energy of the liquid phase and $\Delta\bar{H}_1$ is the partial enthalpy of component 1.

In the special case where a supercritical gas (component 1) is in equilibrium with a nonvolatile solvent (component 2), they assumed that (a) the composition of the nonvolatile solvent in the vapor phase is negligible so that $y_2 \approx 0$, and (b) the solubility of the supercritical component in the liquid is low so that $x_1 \approx 0$. Introducing these two assumptions, Wisniak et al.[28] reduced the aforementioned equation to

$$\left(\frac{\partial x_1}{\partial T}\right)_P \approx -\frac{\Delta\bar{H}_1}{T}\left(\frac{\partial^2\tilde{G}^L}{\partial x_2^2}\right)^{-1}_{T,P} \tag{4}$$

However

$$\left(\frac{\partial^2\tilde{G}^L}{\partial x_2^2}\right)_{T,P} = \frac{\partial \ln\gamma_2}{\partial x_2} - \frac{\partial \ln\gamma_1}{\partial x_2} + \frac{RT}{x_1x_2} \tag{5}$$

Since it was assumed that the supercritical component (component 1) has a low solubility, as $x_1 \to 0$ ($x_2 \to 1$), $\gamma_1 \to \gamma_1^\infty$ and $\gamma_2 \to 1$, Wisniak and coworkers[28] assumed that

$$\left(\frac{\partial^2\tilde{G}^L}{\partial x_2^2}\right)_{T,P,x_1\to 0} \approx \frac{RT}{x_1} \tag{6}$$

By replacing Eq. 6 into Eq. 3 they arrived at

$$\left(\frac{\partial x_1}{\partial T}\right)_{P,x_1\to 0} \approx -\frac{x_1\Delta\bar{H}_1}{RT^2} \tag{7}$$

Since the assumptions involved in the aforementioned derivations also comply closely to the solution of hydrogen in ionic liquids, this equation shows that the temperature dependence of solubility at constant pressure depends only on

Table 3. Solubility (in Mole Fraction) of Various Gases in Two Ionic Liquids

	[bmim][BF_4] at 303 K and 0.1 MPa		[bmim][PF_6] at 283 K and 0.1 MPa	
Component	Solubility, mole fraction	Sign of temperature coefficient of solubility	Solubility, mole fraction	Sign of temperature coefficient of solubility
CO_2	1.6×10^{-2}	–	2.6×10^{-2}	–
C_2H_6	3.1×10^{-3}	–	5.0×10^{-3}	–
CH_4	1.1×10^{-3}	–	1.6×10^{-3}	–
Ar	6.6×10^{-4}	–	1.1×10^{-3}	–
O_2	6.2×10^{-4}	nearly constant	1.1×10^{-3}	–
N_2	5.6×10^{-4}	nearly constant	1.1×10^{-3}	–
CO	5.7×10^{-4}	nearly constant	8.3×10^{-4}	nearly constant
H_2	4.7×10^{-4}	nearly constant	2.8×10^{-4}	+

Data taken from Jacquemin et al.[10,23]

the sign of the heat effect of hydrogen solubility in the ionic liquid ($\Delta\overline{H}_1$). The sign itself can be established using various thermodynamic relations, for example, the relation between gas solubility and the Lennard-Jones potential. Following detailed derivations in which ε_1 symbolizes the Lennard-Jones energy parameter, and k is the Boltzmann's constant, Leites[29] showed that at small values of ε_1/k, corresponding to low-gas solubility, ($\Delta\overline{H}_1$) is positive. Following his calculations, He, H_2, N_2, and O_2 are gases which will cool down upon solution in many solvents. Leites suggested the determining boundary to be near $\varepsilon_1/\varepsilon_2 = 3/7$, where ε_2 is the energy parameter of the solvent. With a numerical value of $\varepsilon_1/k = 59.7$ K, hydrogen has among the lowest values of Lennard-Jones force constants (ε_1/k).[30] When comparing with ε_2/k values of typical solvents, the vast majority being above 200 K, it is evident that hydrogen will have a positive ($\Delta\overline{H}_1$) value upon dissolution in most solvents. Ionic liquids, which are of particular concern in this study, also have very high values of ε_2/k, for example ranging from 365.0 to 375.37 K for [C_n–mim][Tf_2N] with the alkyl side chain varying from C_2 to C_8, respectively.[31] Of course one may argue that in the case of ionic liquids, the errors can be reduced by using an effective Lennard-Jones potential corrected with a term for dipole-induced dipole interactions.[32]

The aforementioned explanations were given with the focus on hydrogen. However, as stated, the cause of this behavior lies in the smallness and the low-intermolecular interactions of the gas molecules. It is, therefore, only reasonable to expect such phenomenon in mixtures of other small gases with small intermolecular forces in ILs as well. In fact this has been observed, for example,[33–35] in the binary systems of O_2 + [bmim][BF_4], Ar + [bmim][PF_6], N_2 and CH_4 each in [emim][BF_4] and [mmim][$MeSO_4$]. It was even seen, just slightly, for the solvation of CO in [bmim][Tf_2N].[36] The relatively constant solubility with temperature of CH_4 in [bmim][Tf_2N] and [hmim][Tf_2N] can also be explained with the rather flat portions of the curves discussed previously.[37,38]

Since small values of energy parameters correlate to lower solubility as stated earlier, a related study by Battino and Clever[39] on the entropy of solution suggested that gases with solubilities less than 10^{-3} mole fraction in conventional solvents generally have positive temperature coefficients of solubility, while those with greater than about 10^{-3} generally have negative temperature coefficients. Table 3, shows the mole fraction of some dissolved gases in [bmim][BF_4] and [bmim][PF_6]. Although, it does not strictly follow the 10^{-3} guideline of Battino and Clever, the trend is definitely observed. It seems that for the case of gases in the ionic liquids in Table 3 in particular, gases with solubilities in the range of 10^{-3} and smaller have negative temperature coefficients, the shift occurs in the region around 10^{-4}, and gases with solubilities less than 10^{-5} will most probably increase their solubility as temperature increases. As further data becomes available for increasing numbers of gas+ionic liquid binaries, it may be possible to indicate a more global empirical transition range for such systems.

Conclusions

Experimental data are presented for the high-pressure solubilities of hydrogen in [bmim][Tf_2N]. These results indicate that hydrogen solubilities are low in this ionic liquid, in fact, about an order of magnitude lower than the corresponding CO_2 solubilities. The pressure-composition curves of hydrogen are more or less linear and are steep. This means that increases in pressure will cause little additional H_2 to dissolve. The P-x curves of H_2 are even steeper than the corresponding P-x curves for CO_2, hence; increasing pressure can result in greater CO_2 dissolution compared to H_2. The temperature dependence of hydrogen solubility is the reverse of CO_2, meaning that hydrogen dissolves better at higher temperatures. Therefore, to obtain the best possible CO_2/H_2 separation efficiency, temperatures should be kept as low as possible.

This "inverse" temperature effect is not only limited to the solution of hydrogen in [bmim][Tf_2N], but seems to be the general rule for hydrogen solubility in all ionic liquids. So far, all the experimental evidence available in ionic liquids has shown this same trend. Because of its importance in future ionic liquid research and development, we have tried to explain this general "inverse" temperature dependency from a thermodynamic point of view. Although we have explained this phenomenon from several different perspectives, the bottom line is that the responsible factor is the extreme lightness and small intermolecular forces of hydrogen molecules. In other words, hydrogen approaches the characteristics of a perfect gas (which consists of completely noninteracting, point-sized molecules). Therefore, such behavior is not only limited to hydrogen but to some other gases which are light and noninteracting as well, for example, oxygen, nitrogen, etc. In addition, we have generalized the behavior of H_2 + IL systems to have type III schematic behavior, according to the classification of Scott-van Konynenburg. This will help predict the qualitative behavior of such systems outside of the range of literature data currently available.

Acknowledgments

This project was part of the Global Climate and Energy Project (GCEP). The authors are grateful to GCEP for the finances. S. Raeissi acknowledges Shiraz University and Delft University of Technology for facilitating the collaboration, and also thanks Dr. Selva Pereda for interesting discussions.

Literature Cited

1. Raeissi S, Peters CJ. A potential ionic liquid for CO_2-separating gas membranes: Selection and gas solubility studies. *Green Chem.* 2009;11:185–192.
2. Gan Q, Rooney D, Xue M, Thompson G, Zou Y. An experimental study of gas transport and separation properties of ionic liquids supported on nanofiltration membranes. *J Mem Sci.* 2006;280:948–956.
3. Jacquemin J, Husson P, Majer V, Costa Gomes MF. Influence of the cation on the solubility of CO_2 and H_2 in ionic liquids based on the bis(trifluoromethylsulfonyl)imide anion. *J Solution Chem.* 2007;36: 9667–979.
4. Scott RL, Van Konynenburg PH. Static properties of solutions: Van der Waals and related models for hydrocarbon mixtures. *Discuss Faraday Soc.* 1970;49:87–97.
5. Raeissi S, Peters CJ. Experimental determination of high-pressure phase equilibria of the ternary system carbon dioxide + limonene + linalool. *J Supercrit Fluids.* 2005;35:10–17.
6. Raeissi S, Peters CJ. Bubble-point pressures of the binary system carbon dioxide + linalool. *J Supercrit Fluids.* 2001;20:221–228.
7. Raeissi S, Peters CJ. Carbon dioxide solubility in the homologous 1-alkyl-3-methylimidazolium bis(trifluoromethylsulfonyl)imide family. *J Chem Eng Data.* 2009;54:382–386.
8. Raeissi S, Florusse L, Peters CJ., Hydrogen solubilities in the IUPAC ionic liquid 1-Hexyl-3-methylimidazolium bis(Trifluoromethylsulfonyl)imide. *J Chem Eng Data.* 2011;56(4):1105–1107.
9. Kumelan J, Kamps APS, Tuma D, Maurer G. Solubility of H_2 in the ionic liquid [bmim][PF6]. *J Chem Eng Data.* 2006;51:11–14.
10. Jacquemin J, Costa Gomes MF, Husson P, Majer V. Solubility of carbon dioxide, ethane, methane, oxygen, nitrogen, hydrogen, argon, and carbon monoxide in 1-butyl-3-methylimidazolium tetrafluoroborate between temperatures 283 K and 343 K and at pressures close to atmospheric. *J Chem Thermodyn.* 2006;38:490–502.
11. Kumelan J, Kamps APS, Tuma D, Maurer G. Solubility of the single gases H_2 and CO in the ionic liquid [bmim][CH_3SO_4]. *Fluid Phase Equilib.* 2007;260:3–8.
12. Schilderman AM, Raeissi S, Peters CJ. Solubility of carbon dioxide in the ionic liquid 1-ethyl-3-methylimidazolium bis(trifluoromethylsulfonyl)imide. *Fluid Phase Equilib.* 2007;260:19–22.
13. Vitu S, Privat R, Jaubert JN, Mutelet F. Predicting the phase equilibria of CO_2 + hydrocarbon systems with the PPR78 model (PR EOS and k_{ij}calculated through a group contribution method). *J Supercrit. Fluids.* 2008;45:1–26.
14. Nieuwoudt I, du Rand M. Measurement of phase equilibria of supercritical carbon dioxide and paraffins. *J Supercrit Fluids.* 2002;22:185–199.
15. Valderrama JO, Rojas RE. Critical properties of ionic liquids. Revisited. *Ind Eng Chem Res.* 2009;48:6890–6900.
16. Körösy F. Two rules concerning solubility of gases and crude data on solubility of krypton. *Trans Faraday Soc.* 1937;33:416–425.
17. McHugh MA, Krukonis VJ. *Supercritical Fluid Extraction: Principles and Practice*. 2nd ed. Butterworth-Heinemann; 1994.
18. Benham A, Katz DL. Vapor-liquid equilibria for hydrogen-light hydrocarbon systems at low temperature. *AIChE J.* 1957;3:33–36.
19. Burriss WL, Hsu NT, Reamer HH, Sage BH. Phase behavior of the hydrogen propane system. *Ind Eng Chem.* 1953;45:210–213.
20. Nichols WB, Reamer HH, Sage BH. Volumetric and phase behavior in the hydrogen-n-hexane system. *AIChE J.* 1957;3:262–267.
21. Brunner E. Fluid mixtures at high pressures I. Phase separation and critical phenomena of 10 binary mixtures of (a gas + methanol). *J Chem Thermodyn.* 1985;17:671–679
22. Jacquemin J, Husson P, Majer V, Costa Gomes MF. Thermophysical properties, low pressure solubilities and thermodynamics of solvation of carbon dioxide and hydrogen in two ionic liquids based on the alkylsulfate anion. *Green Chem.* 2008;10:944–950.
23. Jacquemin J, Husson P, Majer V, Costa Gomes MF. Low-pressure solubilities and thermodynamics of solvation of eight gases in 1-butyl-3-methylimidazolium hexafluorophosphate. *Fluid Phase Equil.* 2006;240:87–95.
24. Wiebe R, Gaddy VL. The solubility of helium in water at 0, 25, 50 and 75° and at pressures to 1000 atmospheres. *J Am Chem Soc.* 1935;57:847–851.
25. Kay WB. Some peculiarities in the P-T border curevs of mixtures of hydrogen and a petroleum naphtha. *Chem Revs.* 1941;29:501–507.
26. Wiebe R, Tremearne TH. The solubility of hydrogen in liquid ammonia at 25,50,75 and 100° and at pressures to 1000 atmospheres *J Am Chem Soc.* 1934:56:2357–2360.
27. Bodner GM. On the misuse of Le Chatelier's principle for the prediction of the temperature dependence of the solubility of salts. *J Chem Ed.* 1980;57:117–119.
28. Wisniak J, Apelblat A, Segura H. The solubility of gases in liquids. *Phys Chem Liq.* 1997;34:125–153.
29. Leites IL. Some trends and a prediction of the solubility of gases in liquids and the heat of dissolution. *Sep Pur Tech.* 1997;12:201–213.
30. Reid RC, Prausnitz JM, Poling BE. *The properties of gases and liquids.* 4th ed. New York: McGraw-Hill, Inc; 1988.
31. Andreu JS, Vega LF. Modeling the solubility behavior of CO_2, H_2, and Xe in [C_n-mim] [Tf_2N] ionic liquids. *J Phys Chem B.* 2008;112:15398–15406.
32. Gibanel F, Lopez MC, Royo FM, Pardo J, Urieta JS. Solubility of 13 non-polar gases (He, Ne, Ar, Kr, Xe, H_2, D_2, N_2, CH_4, C_2H_4, C_2H_6, CF_4, and SF_6,) in 2-methyltetrahydrofuran at 273.15 to 303.15 K and 101.33 kPa partial pressure of gas. *Fluid Phase Equilib.* 1993;87:285–294.
33. Husson-Borg P, Majer V, Costa Gomes MF. Solubilities of oxygen and carbon dioxide in butyl methyl imidazolium tetrafluoroborate as a function of temperature and at pressures close to atmospheric pressure. *J Chem Eng Data.* 2003;48:480–485.
34. Anthony JL, Maginn EJ, Brennecke JF. Solubilities and thermodynamic properties of gases in the ionic liquid 1-n-butyl-3-methylimidazolium hexafluorophosphate. *J Phys Chem B.* 2002;106:7315–7320.
35. Finotello A, Bara JE, Narayan S, Camper D, Noble RD. Ideal gas solubilities and solubility selectivities in a binary mixture of room-temperature ionic liquids. *J Phys Chem B.* 2008;112:2335–2339.
36. Florusse LJ.Raeissi S, Peters CJ. An IUPAC Task Group study: the solubility of carbon monoxide in [hmim][Tf_2N] at high pressures, *J Chem Eng. Data.* 2011;56:4797–4799.
37. Raeissi S, Peters CJ. High pressure phase behavior of methane in 1-butyl-3-methylimidazolium bis(trifluoromethylsulfonyl)imide. *Fluid Phase Equilib.* 2010;294:67–71.
38. Finotello A, Bara JE, Camper D, Noble RD. Room-temperature ionic liquids: temperature dependence of gas solubility selectivity. *Ind Eng Chem Res.* 2008:47:3453–3459.
39. Battino R, Clever HL. The solubility of gases in liquids. *Chem Rev.* 1966;66:395–463.

Manuscript received Aug. 12, 2011, revision received Nov. 16, 2011, and final revision received Jan. 10, 2012.